ELSEVIER

Biochimica et Biophysica Acta 1609 (2003) 109–114

BIOCHIMICA ET BIOPHYSICA ACTA
BBA

www.bba-direct.com

Redox potentials of the oriented film of the wild-type, the E194Q-, E204Q- and D96N-mutated bacteriorhodopsins

Satoru Ueno[a], Akira Shibata[a,*], Ayako Yorimitsu[a], Yoshinobu Baba[a], Naoki Kamo[b]

[a] *Faculty of Pharmaceutical Sciences, Tokushima University, Shomachi-1, Tokushima 770-8505, Japan*
[b] *Faculty of Pharmaceutical Sciences, Hokkaido University, Nishi 6, Kita-ku, Hokkaido, Sapporo 060-0812, Japan*

Received 18 July 2002; received in revised form 22 October 2002; accepted 5 November 2002

Abstract

The redox potentials of the oriented films of the wild-type, the E194Q-, E204Q- and D96N-mutated bacteriorhodopsins (bR), prepared by adsorbing purple membrane (PM) sheets or its mutant on a Pt electrode, have been examined. The redox potentials (V) of the wild-type bR were -470 mV for the 13-*cis* configuration of the retinal Shiff base in bR and -757 mV for the all-*trans* configuration in H_2O, and -433 mV for the 13-*cis* configuration and -742 mV for the all-*trans* configuration in D_2O. The solvent isotope effect ($\Delta V = V(D_2O) - V(H_2O)$), which shifts the redox potential to a higher value, originates from the cooperative rearrangements of the extensively hydrogen-bonded water molecules around the protonated C=N part in the retinal Schiff base. The redox potential of bR was much higher for the 13-*cis* configuration than that for the all-*trans* configuration. The redox potentials for the E194Q mutant in the extracellular region were -507 mV for the 13-*cis* configuration and -788 mV for the all-*trans* configuration; and for the E204Q mutant they were -491 mV for the 13-*cis* configuration and -769 mV for the all-*trans* configuration. Replacement of the Glu^{194} or Glu^{204} residues by Gln weakened the electron withdrawing interaction to the protonated C=N bond in the retinal Schiff base. The E204 residue is less linked with the hydrogen-bonded network of the proton release pathway compared with E194. The redox potentials of the D96N mutant in the cytoplasmic region were -471 mV for the 13-*cis* configuration and -760 mV for the all-*trans* configuration which were virtually the same as those of the wild-type bR, indicating that the D to N point mutation of the 96 residue had no influence on the interaction between the D96 residue and the C=N part in the Schiff base under the light-adapted condition. The results suggest that the redox potential of bR is closely correlated to the hydrogen-bonded network spanning from the retinal Schiff base to the extracellular surface of bR in the proton transfer pathway.

Keywords: Redox potential; Bacteriorhodopsin; Mutant; Shiff base; Hydrogen-bonded network

1. Introduction

Bacteriorhodopsin (bR) transports protons across the membrane upon absorption of light by the retinylidene chromophore. bR consists of seven transmembrane helices with a retinal bound to the ε-amino group of Lys^{216} on the helix via a protonated Schiff base. The Schiff base, and the anionic Asp^{85} and the protonated Asp^{96}, located in the extracellular and cytoplasmic regions, respectively, constitute the main components of the proton pathway. After light excitation, the light-adapted bR undergoes a photocycle with the intermediates $bR \rightarrow h\nu \rightarrow K \rightarrow L \rightarrow M \rightarrow N \rightarrow O$, which is accompanied by vectorial proton transfer [1–4]. Crucial events in the mechanism of proton transport are the retinal Schiff base isomerization from the all-*trans* into the 13-*cis* configuration in the $bR \rightarrow K$ transition, the proton transfer from the Schiff base to Asp^{85} and concomitant proton release into the extracellular medium from the proton release group, Glu^{194} or Glu^{204} in the $L \rightarrow M$ transition, the reprotonation of the Schiff base by Asp^{96} in the $M \rightarrow N$ transition, and the 13-*cis* to all-*trans* reisomerization in the $N \rightarrow O$ transition.

The interhelical cavity is divided by the Schiff base into extracellular and cytoplasmic "half-channels" that together describe the proton transport pathways. The extracellular region contains an extensive hydrogen-bonded network that connects the Schiff base, numerous ionizable residues and many bound water molecules [5,6], whereas the

* Corresponding author. Tel.: +81-88-633-7286; fax: +81-88-633-9507.
E-mail address: ashibata@ph.tokushima-u.ac.jp (A. Shibata).

0005-2736/02/$ - see front matter © 2002 Elsevier Science B.V. All rights reserved.
PII: S0005-2736(02)00660-0

cytoplasmic region is simpler and mostly hydrophobic [7]. The change in this network must be the basis for the coupling that links the protonation of Asp^{85} at one end of this network to the release of a proton to the surface at the other [8,9].

A number of studies performed on mutated bR have indicated that Glu^{194} and Glu^{204} residues are essential elements of the proton release pathway, which appear to be a complex organized into a chain or a hydrogen-bonded network of residues in the extracellular channel [10,11]. The side-chain oxygens of Glu^{194} and Glu^{204} are connected directly through a hydrogen bonding [6,12,13], so that these Glu residues could act as a proton donor/acceptor pair [14] or as a dyad [15]. However, these two Glu side chains do not behave equivalently, as demonstrated by the inhibition of the second increase of the Asp^{85} pK_a during the photocycle in the E194Q mutant but not in the E204Q [16]. The second half of the photocycle of the E204Q mutant is slowed down more than 10-fold compared to the wild-type bR [17].

In the second part of the photocycle, the Schiff base is reprotonated during the M → N transition from Asp^{96} which is located closer to the cytoplasmic side of the membrane. The rate-limiting step in the reprotonation is considered to be the conformational change that brings water molecules into this region to complete it [18,19]. In the N → O transition, Asp^{96} is protonated from the cytoplasmic surface, and coupled to this, the retinal isomerizes from 13-*cis* to the initial all-*trans* configuration [20]. In D96N mutant, reprotonation of the Schiff base is much slow. Recently published three-dimensional structure of bR has demonstrated that virtually no differences between the light-adapted forms of the D96N mutant and the wild-type bR are detected except at the location of the residue change [18].

Recently, we reported that the differential pulse voltammograms of bR in the PM in 0.1 M KCl aqueous solution had one redox peak at − 781 mV for the light-adapted bR and two redox peaks at − 484 and − 781 mV for the dark-adapted bR [21]. The lower potential peak, which was present under both the light and dark conditions, was assigned to the all-*trans* configuration and the higher potential peak under the dark condition was assigned to the 13-*cis* configuration.

In the present study, in order to learn whether the process including the redox transformations of bR is correlated to the hydrogen-bonded network of the proton transport pathway, we examined the solvent isotope effect on the redox potential of the wild-type bR and the redox potential of the E194Q-, E204Q- and D96N-mutated bRs. We detected the redox potentials of the 13-*cis* and all-*trans* configuration of the wild-type, the E194Q-, E204Q- and 96DN-mutated bRs, which were prepared by adsorbing the PM sheets or its mutant on a Pt electrode. The results suggest that the redox potential of bR is closely correlated to the hydrogen-bonded network of the proton transfer pathway.

2. Experimental

The purple membrane (PM) fragments with about 0.5-μm diameter were prepared from *Halobacterium salinarium* strain S-9 cells. The D96N, E194Q and E204Q mutants were isolated after expression in *H. salinarium* as PM patches. The oriented PM film was prepared by the electrophoretic sedimentation technique [22]. Briefly, the PM suspension (160 μM) was filled in the gap (10 mm) between two electrodes and then the electric potential of 400 mV/cm was applied across the electrode. The PM sheets were adsorbed on a Pt electrode (1.0 × 5.0 × 0.1 cm) as the solid support.

The redox potential was measured by the differential pulse voltammetric method (Yanako-P-1100 polarographic analyzer (Kyoto, Japan)). Voltammograms were obtained using a three-electrode circuit (working electrode, electrode deposited PM as reference electrode, Pt plate (0.5 × 5.0 × 0.1 cm); SCE). All potentials in this study are given vs. SCE. Voltammograms of the light- and dark-adapted PM films were measured as follows: the former film was illuminated for 40 min and the latter film was allowed to stand for 40 min in the dark, and then each voltammogram was measured. A 120-W quartz halogen lamp was used as the light source in combination with a HOYA L37 filter as the UV cut filter. All measurements were carried out in the 10 mM KCl aqueous solution (pH. 6.5) under an Ar atmosphere at room temperature.

3. Results and discussion

3.1. Redox potential of bR in the PM film

We previously reported the differential pulse voltammograms of bR in the PM suspended in a 0.1 M KCl aqueous solution in the light-adapted state and the bleached bR which was treated with hydroxylamine under light irradiation [21]. The light-adapted bR showed a redox peak at − 781 mV and the bleached bR showed no redox peak. This indicates that the origin of the redox peak is the retinal chromophoric part bound via a protonated Schiff base to Lys^{216}. Therefore, we concluded that the reducible moiety in bR was attributable to the C=N part of the retinal Schiff base [23].

Fig. 1 (trace a) shows the difference voltammogram of bR in the oriented PM film with and without light illumination, prepared by the electrophoretic sedimentation technique (see Experimental part). The difference voltammogram was obtained by subtracting that of the dark-adapted PM film, which contains all-*trans* and 13-*cis* retinals, from the voltammogram of the light-adapted PM film, which contains all-*trans* retinal. The difference in current (ΔI) between the voltammograms of the light-adapted PM film and the dark-adapted one is caused by the presence of retinal isomer abundance in the PM film. The difference voltammogram for the oriented PM film gave a positive peak at − 757 mV

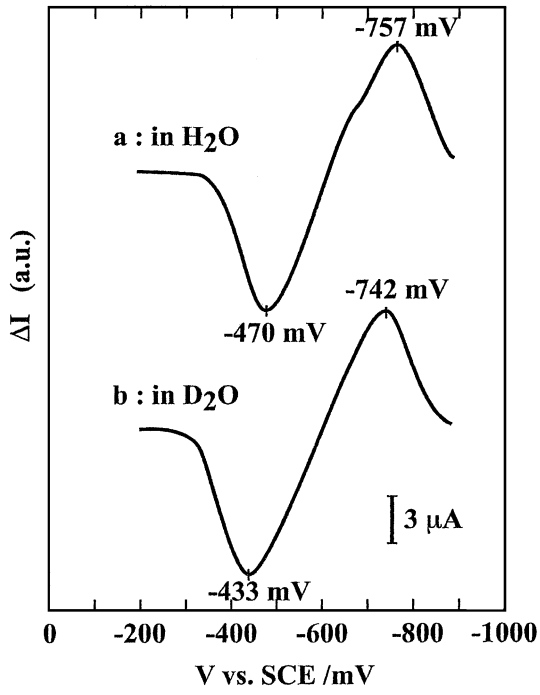

Fig. 1. The difference voltammograms of bR in the oriented PM film on the Pt electrode in H_2O (trace a) and D_2O (trace b). The difference voltammogram was obtained by subtracting that of the dark-adapted PM film from the voltammogram of the light-adapted PM film.

and a negative peak at −470 mV. The positive peak implies that the corresponding redox species contained in the light-adapted PM are far outnumbered, compared with that contained in the dark-adapted PM. The reverse is true for the negative peak. According to the analysis of the redox reaction of the PM suspension in 0.1 M KCl solution [21], the peaks at −757 and −470 mV could be assigned to the all-*trans* and the 13-*cis* configuration, respectively. From the peak area of the difference voltammogram, the ratio of all-*trans* to 13-*cis* form was qualitatively a one-to-one [24]. Taking into account the finding that the redox potential (V = −781 mV) of the retinal-butylamine Schiff base in aqueous solution agreed between the all-*trans* and the 13-*cis* configurations [25], the marked difference in the redox potential between the all-*trans* and the 13-*cis* configurations of the retinal in bR must be caused by the interaction between the chromophore part including the Schiff base and the amino acid residues in the apoprotein. In addition, the results indicate that the protonated C=N bond of the retinal Schiff base for the 13-*cis* configuration is more reducible than that for the all-*trans* configuration.

The ^{15}N NMR study by Hu et al. [26] showed that the dark-adapted bR had a doublet at 143 and 150 ppm, corresponding to all-*trans* isomer and 13-*cis* isomer, respectively, indicating that the electron density on the N atom of the 13-*cis* isomer was lower than the all-*trans* isomer in the dark-adapted bR. According to the FT-IR [27] and Raman spectroscopic studies [28], the C=N stretching vibration sensitively responds to hydrogen-bonding and electrostatic interactions of the Schiff base with its immediate environment. Therefore, the reformation of the NH−X hydrogen-bonding in the retinal binding pocket by transition from the all-*trans* to 13-*cis* form should result in a lowering of the electron density of the C=N bond in the Schiff base, since the NH-acceptor (X) hydrogen-bonding formed for the 13-*cis* configuration of the retinal Schiff base is stronger than that for the all-*trans* configuration [29].

Fig. 2 shows the effect of pH on the redox potential of the light-adapted bR. The pH dependency of the redox potential of bR was quite low (4 mV/pH unit) in the pH range of 3.0 to 10.7. Therefore, the change in the protonation state of bR is considered to be not involved in the redox process described above.

3.2. Solvent isotope effect

We examined the solvent isotope effect on the redox potential of the wild-type bR. The voltammogram profile of bR in the oriented PM film in D_2O showed a positive peak at −742 mV for the redox reaction of the all-*trans* configuration under the light-adapted condition and a negative peak at −433 mV for the 13-*cis* configuration under the dark-adapted condition (Fig. 1, trace b). These values in D_2O are compared with those in H_2O; the solvent isotope effect, $\Delta V(=V(D_2O)-V(H_2O))$, was 15 mV for the all-*trans* configuration and 37 mV for the 13-*cis* configuration, respectively. The replacement of the hydrogen in the hydrogen bonding by deuterium in D_2O shifted the redox potentials of bR to a higher value compared to that in H_2O. This is explained by the electron withdrawing interaction to the protonated C=N bond in D_2O due to the enhancement of the ND−acceptor (X) hydrogen-bonding formed through the

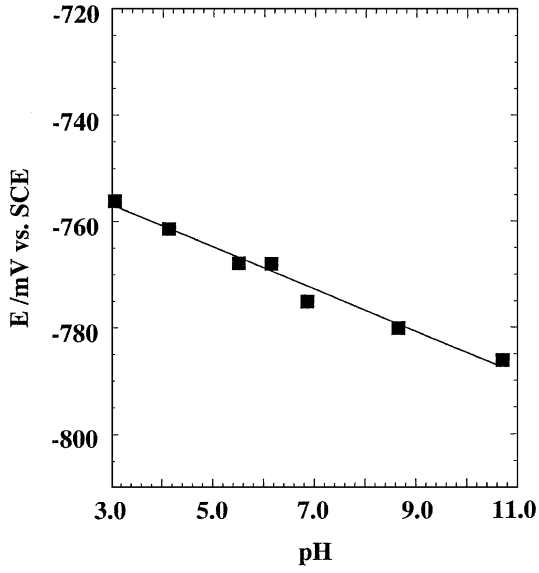

Fig. 2. The effect of pH on the redox potential of the light-adapted bR. The pH dependency of the redox potential of bR was 4 mV per pH unit in the pH range of 3.0 to 10.7.

protonated C=N bond in the Schiff base. The solvent isotope effect was much greater for the 13-*cis* isomer than for the all-*trans* isomer, indicating that the 13-*cis* configuration forms a more enhanced NH–X hydrogen-bonding compared to the all-*trans* configuration [29]. The results suggest that the redox reaction of bR in the PM is closely associated with an extensive hydrogen-bonded network that connects the Schiff base.

3.3. Redox potentials of the E194Q and E204Q mutants

The replacement of Glu^{194} or Glu^{204} by Gln alters the proton-release kinetics [6]. The crystallographic structure of bR has demonstrated that a three-dimensional network of hydrogen-bonded side chains and water molecules connects the active site of the bR state with the residues such as Arg^{82}, Glu^{194} and Glu^{204} that participate in the release of a proton to the extracellular surface upon protonation of Asp^{85} [12,13]. A mutation of any one of three residues, Arg^{82}, Glu^{194}, or Glu^{204}, inhibits fast proton release at neutral pH and slows down the proton release from Asp^{85} [14,30].

Fig. 3 shows the difference voltammograms of the E194Q and E204Q mutants. The redox potential values (V) of the E194Q mutant, which is located in the extracellular half-channel, were −507 mV for the 13-*cis* configuration and −788 mV for the all-*trans* configuration (trace a), and for the E204Q mutant they were −491 mV for the 13-*cis* configuration and −769 mV for the all-*trans* configuration (trace b). The redox potentials of these mutants

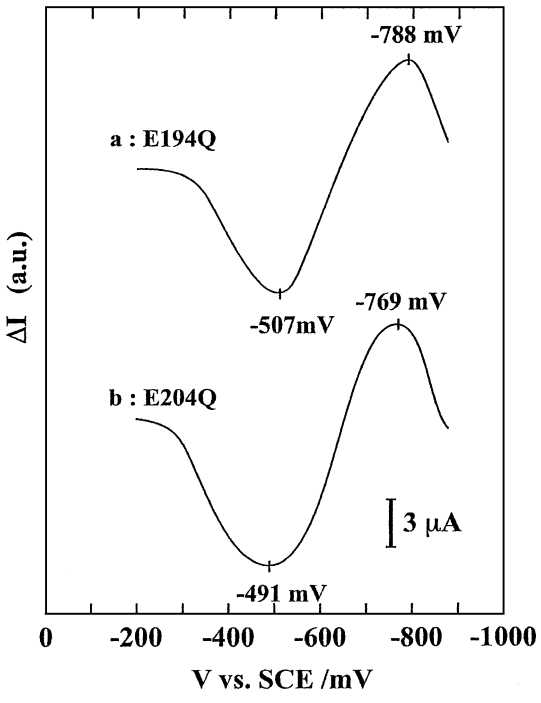

Fig. 3. The difference voltammograms of the E194Q- and E204Q-mutated bRs with and without light illumination.

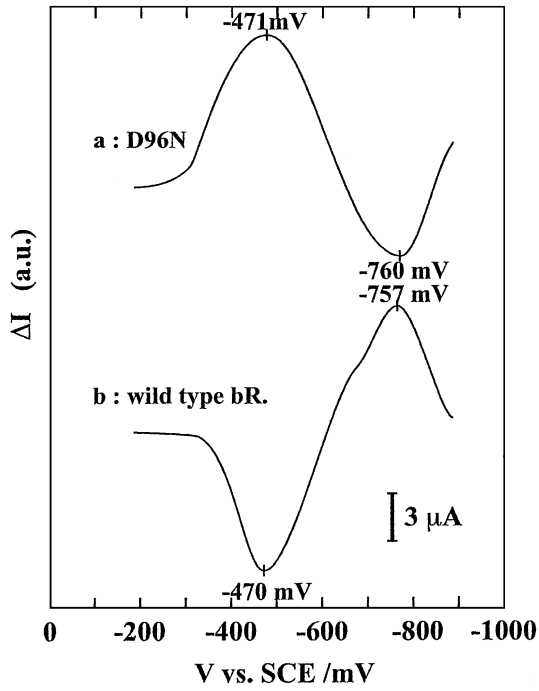

Fig. 4. The difference voltammograms of the D96N-mutated bR (trace a) and the wild-type bR (trace b) with and without light illumination.

are compared with that of the wild-type bR (Fig. 1, trace a). The mutation effects ($\Delta V = V$(mutant) − V(bR)) for the E194Q mutant were −37 mV for the 13-*cis* configuration and −31 mV for the all-*trans* configuration, and for the E204Q mutant they were −21 mV for the 13-*cis* configuration and −12 mV for the all-*trans* configuration. These mutants shifted the redox potential to a lower value compared to that of the wild-type bR, indicating the decrease in the electron withdrawing interactions to the C=N part in the retinal Schiff-base moieties. The difference voltammogram profile also showed a broadening of the redox peaks for the E194Q and E204Q mutants (Fig. 3). The half-widths of the negative peak assigned to the 13-*cis* configuration were 140 mV for the wild-type bR (Fig. 1, trace a), 200 mV for the E194Q mutant and 270 mV for the E204Q mutant. The half-width is defined as the width at 50% of the peak height of the current. The replacement of Glu^{194} or Glu^{204} residues by Gln decreased the hydrogen-bonding ability, because the Gln side chain only binds one hydrogen-bonded water molecule, whereas Glu binds two. Therefore, the increase in the half-width of the redox peak for these mutants may be related to the weakening or fluctuation of the hydrogen-bonded network formed through the C=N part of the Schiff base. These results provide evidence that both Glu^{194} and Glu^{204} link with the hydrogen-bonded network that connects the retinal Schiff base. However, these two Glu side chains seem not to behave equivalently in the proton translocation pathway, as demonstrated by the difference in the redox potential of these mutants [31]. The E204 mutant is less linked with the hydrogen-bonded network compared with the E194 mutant.

3.4. D96N

The cytoplasmic region does not contain an interconnected hydrogen-bonded network in the bR state. The most severe structural changes during the photocycle are in the cytoplasmic portions of helices F and G, which result in an enlargement of the cavities thereby enabling the inward and outward diffusion of water molecules [20]. Therefore, the reprotonation of the Schiff base from Asp^{96} as well as the reprotonation of Asp^{96} itself is only possible by fluctuating water molecules and the motions of the amino acid side chains [32].

The difference voltammogram of the D96N mutant is shown in Fig. 4 (trace a) together with that of the wild-type bR (trace b). The redox potentials of the D96N mutant under the light-adapted condition were −471 mV for the 13-*cis* configuration and −760 mV for the all-*trans* configuration. Virtually no differences in the redox potentials between the light-adapted forms of the D96N mutant and the wild-type bR were detected. This supports the X-ray diffraction data in which the light-adapted forms of the D96N mutant do not differ from the wild-type protein of bR in the three-dimensional structure in the bR state [12]. In addition, the sign of the peak currents at $V=-471$ mV and at $V=-760$ mV in the voltammogram profile of the D96N mutant were reversed with that (the positive peak at −757 mV and negative peak at −470 mV) of the wild-type bR, indicating that under the light-adapted condition, the D96N mutant is in the 13-*cis* configuration (the positive peak at −471 mV). When Asp^{96} is replaced by Asn, the photocycle is slowed down by 100- to 500-fold under neutral pH compared to the wild-type bR due to accumulation of the M intermediate which is in the 13-*cis* configuration [33,34]. Therefore, the redox potential of the D96N mutant is considered to be for the 13-*cis* configuration under the continuous illumination.

Table 1
The redox potentials of the 13-*cis* and all-*trans* configurations of the wild-type, the E194Q-, E204Q- and D96N-mutated bRs

bR	13-*cis* form (mV)	ΔV^{cis} (D_2O-H_2O)[a] (mV)	all-*trans* form (mV)	ΔV^{trans} (D_2O-H_2O)[a] (mV)
WT bR (in H_2O)	−470	–	−757	–
WT bR (in D_2O)	−433	37	−742	15
		ΔV^{cis} (Mu-Wt)[b]		ΔV^{trans} (Mu-Wt)[b]
E194Q	−507	−37	−788	−31
E204Q	−491	−21	−769	−12
D96N	−471	−1	−760	−3

[a] ΔV^{cis} (D_2O-H_2O) and ΔV^{trans} (D_2O-H_2O): the solvent isotope effects on the redox potential of bR, which are obtained by subtracting that in H_2O from the redox potential (mV) of the wild-type bR with the 13-*cis* or all-*trans* configuration in D_2O.

[b] ΔV^{cis} (Mu − Wt) and ΔV^{trans} (Mu − Wt): the mutation effects on the redox potential of bR, which obtained by subtracting that of the wild-type bR from the redox potential (mV) of the mutants with the 13-*cis* or all-*trans* configuration.

4. Conclusions

This paper describes the solvent isotope effect on the redox potential of the wild-type bR and the redox potential of the D96N, E194Q and E204Q mutants. The obtained redox potentials are summarized in Table 1. The replacement of the hydrogen in the hydrogen bonding by deuterium in D_2O increased the redox potentials of bR. The solvent isotope effect is explained by an electron withdrawing interaction to the protonated C=N bond in the retinal Schiff base in D_2O due to the enhancement of the ND−acceptor (X) hydrogen-bonding formed through the protonated C=N bond. The redox potential of bR was much larger for the 13-*cis* configuration than that of the all-*trans* configuration. The E194Q and E204Q mutants shifted the redox potential to a smaller value compared to that of the wild-type bR. In addition, the redox potential of the E204Q was smaller than that of the E194Q. The replacement of Glu^{194} or Glu^{204} residues by Gln weakened the electron withdrawing interaction to the protonated C=N bond in the retinal Schiff base. The E204 residue is less linked with the hydrogen-bonded network of the proton release pathway compared with E194. The redox potentials of the D96N mutant indicated that the D to N point mutation of 96 residue had virtually no influence on the interaction between the D96 residue and the C=N part in the Schiff base under the light-adapted condition. In this study, the main new results are as follows: (1) the redox potentials of the 13-*cis* and all-*trans* configurations of the wild-type, the D96N-, E194Q- and E204Q-mutated bRs were detected, and (2) the redox potential of bR is closely correlated to the hydrogen-bonded network spanning from the retinal Schiff base to the extracellular surface of bR in the proton transfer pathway.

Acknowledgements

We gratefully thank Dr. Janos K. Lanyi for the generous gift of bR mutants. This work was supported in part by a research grant from Faculty of Pharmaceutical Sciences, The University of Tokushima.

References

[1] D. Oesterhelt, J. Tittor, E. Bamberg, A unifying concept for ion translocation by retinal proteins, J. Bioenerg. Biomembranes 24 (1992) 181–191.
[2] N. Grigorieff, T.A. Ceska, K.H. Downing, J.M. Baldwin, R. Henderson, Electron-crystallographic refinement of the structure of bacteriorhodopsin, J. Mol. Biol. 259 (1996) 393–421.
[3] J.K. Lanyi, Mechanism of ion transport across membranes. Bacteriorhodopsin as a prototype for proton pumps, J. Biol. Chem. 272 (1997) 31209–31212.

[4] D. Oesterhelt, The structure and mechanism of the family of retinal proteins from halophilic archaea, Curr. Opin. Struck. Biol. 8 (1998) 489–500.
[5] I. Rousso, N. Friedman, A. Lewis, M. Sheves, Evidence for a controlling role of water in producing the native bacteriorhodopsin structure, Biophys. J. 73 (1997) 2081–2089.
[6] R. Rammelsberg, G. Huhn, M. Lubben, K. Gerwert, Bacteriorhodopsin's intramolecular proton-release pathway consists of a hydrogen-bonded network, Biochemistry 37 (1998) 5001–5009.
[7] E. Pebay Peyroula, G. Rummel, J.P. Rosenbusch, E.M. Landau, X-ray structure of bacteriorhodopsin at 2.5 angstroms from microcrystals grown in lipidic cubic phases, Science 277 (1997) 1676–1681.
[8] S.P. Balashov, E.S. Imasheva, R. Govindjee, T.G. Ebrey, Titration of aspartate-85 in bacteriorhodopsin: what it says about chromophore isomerization and proton release, Biophys. J. 70 (1996) 473–481.
[9] H.-T. Richter, L.S. Brown, R. Needleman, J.K. Lanyi, A linkage of the p*K*a's of Asp-85 and Glu-204 forms part of the reprotonation switch of bacteriorhodopsin, Biochemistry 35 (1996) 4054–4062.
[10] I.V. Kalaidzidis, I.N. Belevich, A.D. Kaulen, Photovoltage evidence that Glu-204 is the intermediate proton donor rather than the terminal proton release group in bacteriorhodopsin, FEBS Lett. 434 (1998) 197–200.
[11] S.P. Balashov, M. Lu, E.S. Imasheva, R. Govindjee, T.G. Ebrey, B. Othersen III, Y.I. Chen, R.K. Crouch, D.R. Menick, The proton release group of bacteriorhodopsin controls the rate of the final step of its photocycle at low pH, Biochemistry 38 (1999) 2026–2039.
[12] H. Luecke, B. Schobert, H.-T. Richter, J.-P. Cartailler, J.K. Lanyi, Structure of bacteriorhodopsin at 1.55 A resolution, J. Mol. Biol. 291 (1999) 899–911.
[13] K. Mitsuoka, T. Hirai, K. Murata, A. Miyazawa, A. Kidera, Y. Kimura, Y. Fujiyoshi, The structure of bacteriorhodopsin at 3.0 a resolution based on electron crystallography: implication of the charge distribution, J. Mol. Biol. 286 (1999) 861–882.
[14] A.K. Dioumaev, L.S. Brown, R. Needleman, J.K. Lanyi, Partitioning of free energy gain between the photoisomerized retinal and the protein in bacteriorhodopsin, Biochemistry 37 (1998) 9889–9893.
[15] L.-O. Essen, R. Siegert, W.D. Lehmann, D. Oesterhelt, Lipid patches in membrane protein oligomers: crystal structure of the bacteriorhodopsin–lipid complex, Proc. Natl. Acad. Sci. U. S. A. 95 (1998) 11673–11678.
[16] T. Lazarova, C. Sanz, E. Querol, E. Padros, Fourier transform infrared evidence for early deprotonation of Asp85 at alkaline pH in the photocycle of bacteriorhodopsin mutants containing E194Q, Biophys. J. 78 (2000) 2022–2030.
[17] S. Misra, R. Govindjee, T.G. Ebrey, N. Chen, J.-X. Ma, R.K. Crouch, Proton uptake and release are rate-limiting steps in the photocycle of the bacteriorhodopsin mutant E204Q, Biochemistry 36 (1997) 4875–4883.
[18] H. Luecke, B. Schobert, J.-P. Cartailler, H.-T. Richter, A. Rosengarth, R. Needleman, J.K. Lanyi, Coupling photoisomerization of retinal to directional transport in bacteriorhodopsin, J. Mol. Biol. 300 (2000) 1237–1255.
[19] J.K. Lanyi, Crystallographic studies of the conformational changes that drive directional transmembrane ion movement in bacteriorhodopsin, Biochim. Biophy. Acta 1459 (2000) 339–345.
[20] A.K. Dioumaev, L.S. Brown, R. Needleman, J.K. Lanyi, Coupling of the reisomerization of the retinal, proton uptake, and reprotonation of Asp-96 in the N photointermediate of bacteriorhodopsin, Biochemistry 40 (2001) 11308–11317.
[21] S. Ueno, A. Shibata, Y. Ito, Redox potential of bacteriorhodopsin in purple membrane determined by differential pulse voltammetry, Chem. Pharm. Bull. 46 (1998) 1944–1945.
[22] A.A. Kononenko, E.P. Lukashev, A.V. Maksimychev, S.K. Chamorovskii, A.B. Rubin, S.F. Timashev, L.N. Chekulaeva, Oriented purple-membrane films as a probe for studies of the mechanism of bacteriorhodopsin functioning: I. The vectorial character of the external electric-field effect on the dark state and the photocycle of bacteriorhodopsin, Biochim. Biophys. Acta 850 (1986) 162–169.
[23] S. Druckmann, R. Renthal, M. Ottolenghi, W. Stoeckenius, The radiolytic reduction of the Schiff base in bacteriorhodopsin, Photochem. Photobiol. 40 (1984) 647–651.
[24] M.J. Pettei, A.P. Yudd, K. Nakanishi, R. Henselman, W. Stoeckenius, Identification of retinal isomers isolated from bacteriorhodopsin, Biochemistry 16 (1977) 1955–1959.
[25] B. Czochralska, M. Szweykowska, N.A. Dencher, D. Shugar, Electrochemical studies on *trans*- and *cis*-retinal and bacteriorhodopsin, Bioelectrochem. Bioenerg. 5 (1978) 713–722.
[26] J.G. Hu, B.Q. Sun, A.T. Petkova, R.G. Griffin, J. Herzfeld, The predischarge chromophore in bacteriorhodopsin: a ^{15}N solid-state NMR study of the L photointermediate, Biochemistry 36 (1997) 9316–9322.
[27] T. Baasov, N. Friedman, M. Sheves, Factors affecting the C=N stretching in protonated retinal Schiff base: a model study for bacteriorhodopsin and visual pigments, Biochemistry 26 (1987) 3210–3217.
[28] S. Gerscher, M. Mylrajan, P. Hildebrandt, M.H. Baron, R. Muller, M. Engelhard, Chromophore-anion interactions in halorhodopsin from *Natronobacterium pharaonis* probed by time-resolved resonance Raman spectroscopy, Biochemistry 36 (1997) 11012–11020.
[29] J. Terner, C.L. Hsieh, M.A. El-Sayed, Time-resolved resonance Raman characterization of the bL550 intermediate and the two dark-adapted bRDA/560 forms of bacteriorhodopsin, Biophys. J. 26 (1979) 527–541.
[30] L.S. Brown, J. Sasaki, H. Kandori, A. Maeda, R. Needleman, J.K. Lanyi, Glutamic acid 204 is the terminal proton release group at the extracellular surface of bacteriorhodopsin, J. Biol. Chem. 270 (1995) 27122–27126.
[31] C. Zscherp, R. Schlesinger, J. Heberle, Time-resolved FT-IR spectroscopic investigation of the pH-dependent proton transfer reactions in the E194Q mutant of bacteriorhodopsin, Biochem. Biophys. Res. Commun. 273 (2001) 57–63.
[32] N.A. Dencher, H.J. Sass, G. Buldt, Water and bacteriorhodopsin: structure, dynamics, and function, Biochim. Biophys. Acta 1460 (2000) 192–203.
[33] H. Otto, T. Marti, M. Holz, T. Mogi, M. Lindau, H.G. Khorana, M.P. Heyn, Aspartic acid-96 is the internal proton donor in the reprotonation of the Schiff base of bacteriorhodopsin, Proc. Natl. Acad. Sci. U. S. A. 86 (1989) 9228–9232.
[34] A. Miller, D. Oesterhelt, Kinetic optimization of bacteriorhodopsin by aspartic acid 96 as an internal proton donor, Biochim. Biophys. Acta 1020 (1990) 57–64.